

their equivalents evaluated on the basis of the smallest resolved scales. The spectrum of the solution based on this hypothesis is therefore broken down into three bands: the largest resolved scales, the smallest resolved scales (*i.e.* the test field), and the unresolved scales (see Fig. 4.14).

This statistical consistency can be interpreted in two complementary ways. The first uses the energy cascade idea. That is, the unresolved scales and the smallest resolved scales have a common history due to their interactions with the largest resolved scales. The classical representation of the cascade has it that the effect of the largest resolved scales is exerted on the smallest resolved scales, which in turn influences the subgrid scales, which are therefore indirectly forced by the largest resolved scales, but similarly to the smallest. The second interpretation is based on the idea of coherent structures. These structures have a non-local frequency signature<sup>9</sup>, *i.e.* they have a contribution on the three spectral bands considered. Scale similarity is therefore associated with the fact that certain structures appear in each of the three bands, inducing a strong correlation of the field among the various levels of decomposition.

**Extended Hypothesis.** This hypothesis was generalized by Liu *et al.* [200] (see [228] for a more complete discussion) to a spectrum split into an arbitrary number of bands, as illustrated in Fig. 6.1. The scale similarity hypothesis is then re-formulated for two consecutive spectrum bands, with the consistent forcing being associated with the low frequency band closest to those considered. Thus the specific elements of the tensors constructed from the velocity field  $u^n$  and their analogous elements constructed from  $u^{n+1}$  are assumed to be the same. This hypothesis has been successfully verified in experiments in the case of a jet turbulence [200] and plane wake turbulence [258]. Liu *et al.* have also demonstrated that scale similarity persists during rapid straining [199].

### 6.4.2 Scale Similarity Models

This section presents the structural models constructed on the basis of the scale similarity hypothesis. All of them make use of a frequency extrapolation technique: the subgrid tensor is approximated by an analogous tensor computed from the highest resolved frequencies. The following are described:

1. Bardina's model (p.179) in which the subgrid tensor is computed by applying the analytical filter a second time and thereby evaluating the

<sup>9</sup> This is due to the fact that the variations of the velocity components associated with a vortex cannot be represented by a monochromatic wave. For example, the Lamb-Oseen vortex tangential velocity radial distribution is:

$$U_\theta = \frac{q}{r} (1 - e^{-r^2}) \quad ,$$

where  $r$  is the distance to the center and  $q$  the maximum vorticity.

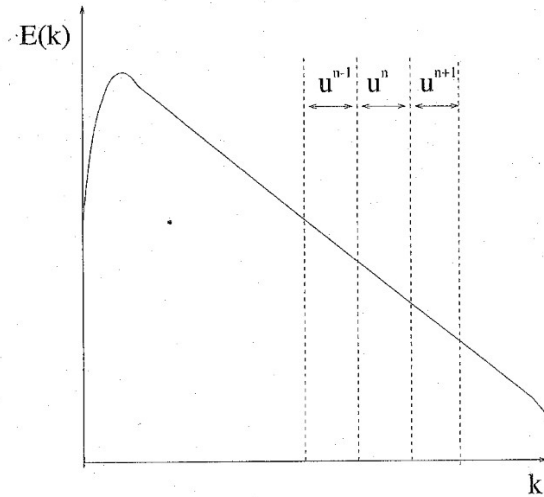


Fig. 6.1. Spectral decomposition based on the extended scale similarity hypothesis.

2. Filtered Bardina model (p.180), which is an improvement on the previous one. By construction, the subgrid tensor is a filtered quantity, which results in the application of a convolution product and is therefore non-local in the sense that it incorporates all the information contained in the support of the filter convolution kernel. It is proposed in this model to cover this non-local character by applying the filter to the modeled subgrid tensor.
3. Liu-Meneveau-Katz model (p.181), which generalizes the Bardina model to the use of two consecutive filters of different shapes and cutoff frequencies, for computing the small scale fluctuations. This model can therefore be used for any type of filter.
4. The dynamic similarity model (p.182), which can be used to compute the intensity of the modeled subgrid stresses by a dynamic procedure, whereas in the previous cases this intensity is prescribed by hypotheses on the form of the energy spectrum.

**Bardina Model.** Starting with the hypothesis, Bardina, Ferziger, and Reynolds [13] proposed modeling the  $C$  and  $R$  terms of the Leonard decomposition by a second application of the filter that was used to separate the scales. We furthermore have the approximation:

$$\overline{\phi\psi} \simeq \overline{\phi} \overline{\psi} \quad , \quad (6.88)$$

which allows us to say:

The backward energy cascade is modulated by controlling the sign and amplitude of the product  $f(I_{LS})I_{LS}$ . The authors considered a number of choices. The first is:

$$f(I_{LS}) = \begin{cases} 1 & \text{if } I_{LS} \geq 0 \\ 0 & \text{otherwise} \end{cases} \quad (6.102)$$

This solution makes it possible to cancel out the representation of the backward cascade completely by forcing the model to be strictly dissipative. One drawback to this is that the function  $f$  is discontinuous, which can generate numerical problems. A second solution that is continuous consists in taking:

$$f(I_{LS}) = \begin{cases} I_{LS} & \text{if } I_{LS} \geq 0 \\ 0 & \text{otherwise} \end{cases} \quad (6.103)$$

One last positive, continuous, upper-bounded solution is of the form:

$$f(I_{LS}) = \begin{cases} (1 - \exp(-\gamma I_{LS}^2)) & \text{if } I_{LS} \geq 0 \\ 0 & \text{otherwise} \end{cases}, \quad (6.104)$$

in which  $\gamma = 10$ .

**Dynamic Similarity Model.** A dynamic version of the Liu–Meneveau–Katz model (6.95) was also proposed [200] for which the constant  $C_1$  will no longer be set arbitrarily. To compute this model, we introduce a third level of filtering identified by  $\hat{\cdot}$ . The  $Q$  analogous to tensor  $\mathcal{L}^m$  for this new level of filtering is expressed:

$$Q_{ij} = (\widehat{\widehat{u}_i \widehat{u}_j} - \widehat{\widehat{u}_i} \widehat{\widehat{u}_j}) \quad (6.105)$$

The Germano–Lilly dynamic procedure, based here on the difference:

$$M_{ij} = f(I_{QS})Q_{ij} - f(I_{LS})\mathcal{L}_{ij}^m, \quad (6.106)$$

where

$$I_{QS} = \frac{Q_{mn}\widehat{\widehat{S}}_{mn}}{|Q|\widehat{\widehat{S}}}, \quad (6.107)$$

yields:

$$C_1 = \frac{\mathcal{L}_{lk}^m M_{lk}}{M_{pq} M_{pq}} \quad (6.108)$$

### 6.4.3 A Bridge Between Scale Similarity and Approximate Deconvolution Models. Generalized Similarity Models

The Bardina model can be interpreted as a particular case of the approximate deconvolution based models described in Sect. 6.1.

Using the second order differential approximation

$$\bar{\phi} = \phi + \frac{\alpha^{(2)}}{2} \frac{\partial^2 \phi}{\partial x^2}, \quad (6.109)$$

the Bardina model (6.92) is strictly equivalent to the second order gradient model given by relations (6.13) and (6.14).

It can also be derived using the iterative deconvolution procedure: a zeroth-order truncation in (6.27) is used to recover relation (6.88), while a first-order expansion is employed to derive (6.89).

The Bardina model then appears as a low-order formal expansion model for the subgrid tensor. Generalized scale similarity models can then be defined using higher-order truncations for the formal expansion [119]. They are formulated as

$$\tau_{ij} = (\overline{G_d^{-1} \star \bar{u}_i})(\overline{G_d^{-1} \star \bar{u}_j}) - (\overline{G_d^{-1} \star \bar{u}})_i - (\overline{G_d^{-1} \star \bar{u}})_j, \quad (6.110)$$

where  $G_d^{-1} \star$  designates the approximate deconvolution operator, defined using equation (6.9) or equation (6.27).

## 6.5 Mixed Modeling

### 6.5.1 Motivations

The structural models based on the scale similarity idea, and the functional models, each have their advantages and disadvantages that make them complementary:

- The functional models, generally, correctly take into account the level of the energy transfers between the resolved scales and the subgrid modes. However, their prediction of the subgrid tensor structure, *i.e.* its eigenvectors, is very poor.
- The models based on the scale-similarity hypothesis or an approximate deconvolution procedure generally predict well the structure of the subgrid tensor better (and then are able to capture anisotropic effects and disequilibrium), but are less efficient for dealing with the level of the energy transfers.